NREL
NATIONAL RENEWABLE ENERGY LABORATORY

Oscillation Damping: A Comparison of Wind and Photovoltaic Power Plant Capabilities

Preprint

M. Singh, A. Allen, E. Muljadi, and V. Gevorgian
National Renewable Energy Laboratory

To be presented at the IEEE Symposium on Power Electronics and Machines for Wind and Water Applications
Milwaukee, Wisconsin
July 24–26, 2014

NREL is a national laboratory of the U.S. Department of Energy
Office of Energy Efficiency & Renewable Energy
Operated by the Alliance for Sustainable Energy, LLC

This report is available at no cost from the National Renewable Energy Laboratory (NREL) at www.nrel.gov/publications.

Conference Paper
NREL/CP-5D00-62260
July 2014

Contract No. DE-AC36-08GO28308

This report is available at no cost from the National Renewable Energy Laboratory (NREL) at www.nrel.gov/publications.

Available electronically at http://www.osti.gov/scitech

Available for a processing fee to U.S. Department of Energy and its contractors, in paper, from:

U.S. Department of Energy
Office of Scientific and Technical Information
P.O. Box 62
Oak Ridge, TN 37831-0062
phone: 865.576.8401
fax: 865.576.5728
email: mailto:reports@adonis.osti.gov

Available for sale to the public, in paper, from:

U.S. Department of Commerce
National Technical Information Service
5285 Port Royal Road
Springfield, VA 22161
phone: 800.553.6847
fax: 703.605.6900
email: orders@ntis.fedworld.gov
online ordering: http://www.ntis.gov/help/ordermethods.aspx

Cover Photos: (left to right) photo by Pat Corkery, NREL 16416, photo from SunEdison, NREL 17423, photo by Pat Corkery, NREL 16560, photo by Dennis Schroeder, NREL 17613, photo by Dean Armstrong, NREL 17436, photo by Pat Corkery, NREL 17721.

NREL prints on paper that contains recycled content.

Oscillation Damping: A Comparison of Wind and Photovoltaic Power Plant Capabilities

M .Singh, A. Allen, E. Muljadi, and V. Gevorgian

Abstract—**This paper investigates the potential for wind power plants (WPPs) and photovoltaic power plants (PVPPs) to damp inter-area oscillations. Inter-area oscillations may be the result of a single or a group of generators oscillating against another group of generators across a weak transmission link. If poorly damped, these power system oscillations can cause system instability and potentially lead to blackouts. Power conversion devices, particularly megawatt-scale converters that connect wind turbines and PVPPs to the grid, could be used to damp these oscillations by injecting power into the system out of phase with the potentially unstable mode. Over time, the net energy injection is near zero; therefore, providing this "static damping" capability is not expected to affect annual energy production. However, WPPs and PVPPs have different capabilities due to the inherent physical nature of these plants. WPPs have some energy stored in the rotating masses of the turbines, whereas PVPPs have no such stored energy. Thus, the challenge to provide oscillation damping services will have to be approached differently for WPPs and PVPPs. This work compares and contrasts strategies for providing oscillation damping services from WPPs and PVPPs.**

Kundur's well-known, two-area, four-generator system is modeled in PSCAD/EMTDC. The WPP and PVPP models are based on the Western Electricity Coordination Council (WECC) standard models. Controllers to damp inter-area oscillations are developed and added to the WECC WPP and PVPP models, and their effects are studied. Analysis is performed on the data generated by the simulations.

***Index Terms*—wind power generation, photovoltaic power generation, power system oscillations, power system stability**

I. INTRODUCTION

VARIABLE generation (VG) penetration levels are increasing throughout the United States. This trend is expected to continue in the coming decades [1]. In certain regions of the United States, peak penetration levels can approach 30% [2]. At these penetration levels, in many cases it is expected that VG such as wind power and photovoltaic (PV) power will displace conventional generation. This displacement may be permanent as a result of conventional plant retirements based on emissions- or age-related concerns and because utilities may prefer to install VG instead of new conventional generation [3,4]. This displacement of conventional synchronous generation by asynchronous VG will have significant stability impacts. In this paper, we focus on inter-area oscillation modes in particular. In the literature, numerous simulation-based studies have been conducted, with specific regard to wind power, with inconclusive results suggesting that the damping of modes may be improved or worsened by wind [5]-[8]. The consensus appears to be that wind power plants (WPPs) do not participate directly in oscillation modes, but their presence leads to the displacement of conventional plant inertia and other topology changes that have the potential to influence the oscillation modes [8]. However, these papers study the passive effects of wind integration rather than active attempts to damp out oscillations. With regard to the effects of photovoltaic power plants (PVPPs) on system modes, the community has not yet generated much literature due to low PV penetration levels and the assumption that PV integration would be a distribution system issue rather than a transmission system issue.

In our present work, we model a familiar two-area test system [9] with an additional WPP. To study the effects of PV, we replace the WPP in our model with a PVPP of equal megawatt rating (204 MW each). We also add an additional oscillation damping controller in each case to directly influence modes. The two-area system model is a time domain model developed using the PSCAD/EMTDC platform [10]. This platform was chosen for its short simulation time step, giving insight into any dynamics that may appear. This platform has been used before for two-area stability analyses [11]. The output from the simulations can be filtered and down-sampled to simulate phasor measurement unit (PMU) data. The WPP model is based on the Western Electricity Coordinating Council (WECC) Wind Generator Modeling Group's standard model for Type 3 (doubly-fed induction generator, or DFIG) WPPs [12]. The PVPP model is also based on the WECC standard model [13]. The standard models are ported to PSCAD/EMTDC based on the work reported in [14]. Additional controls for inter-area oscillation damping have been added to the standard models to inject power into the system out of phase with the potentially unstable mode. A detailed explanation of the model development is provided in Section II.

In the work presented here, a method based on the Yule-Walker power spectral density (PSD) calculation algorithm [15] is applied to analyze the simulated PMU data generated by the model. A description of the method is provided in Section II. The effectiveness of the damping controls for different WPP and PVPP output levels is investigated with

M. Singh, A. Allen, E. Muljadi, and V. Gevorgian are with National Renewable Energy Laboratory, Golden, CO, USA (e-mail: eduard.muljadi@nrel.gov).

respect to changes in oscillation modes. These scenarios are discussed in detail in Section IV. The results of the analysis indicate that the oscillation damping controller is able to influence modes by improving the damping of the system; however, it has to be tuned for one particular mode, and its effects on other modes are difficult to predict. Detailed results and discussion are provided in Section V.

II. Model Development

The model used for these simulations was developed in three stages. In the first stage, a model of the two-area system was developed in PSCAD/EMTDC. In the next stage, a model of the WECC standard WPP was developed and integrated into the two-area system model. The original WECC model was intended for phasor-based modeling software such as PSLF or PSS/E [16]. In our work, we use a time-domain PSCAD/EMTDC equivalent of the WECC model (discussed in detail in [14]). In the third stage, an oscillation damping controller was developed and added to the model.

A. Two-Area System Model

A one-line diagram of the two-area system is shown in Fig. 1. The base system is symmetrical in terms of generation and line impedance. The model parameters are taken from [9]. In steady-state conditions with no wind, there is a 400-MW transfer from Area 1 to Area 2 across the weak transmission tie between the areas. It should be noted that in our model power system stabilizers and automatic generation control are not included; however, each generator's excitation system and governor are modeled. PSCAD/EMTDC parameters for modeling generators and controls not provided in [9] are left at default values when reasonable. For electromechanical transients, reflection of traveling waves at transmission line ends is not important; hence, instead of using traveling-wave or frequency-dependent transmission line models, a coupled-pi transmission line representation is used to model each of the transmission lines in the system.

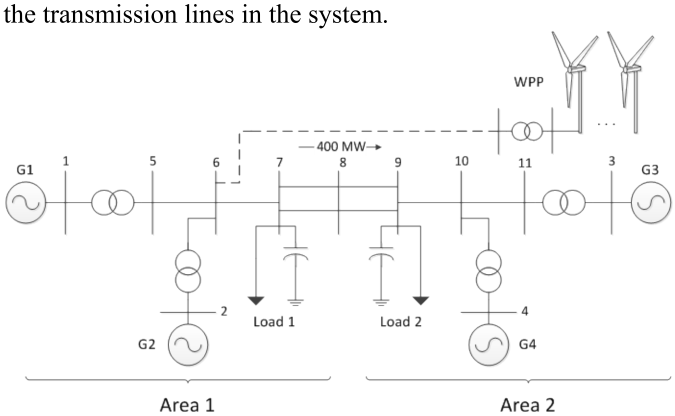

Fig. 1. Two-area system from Kundur [9] with an additional WPP.

B. WPP Model

The WPP model is a PSCAD/EMTDC equivalent of the DFIG WPP model developed by the WECC Wind Generator Modeling Group. Fig. 2 illustrates a schematic of the WECC DFIG WPP model framework.

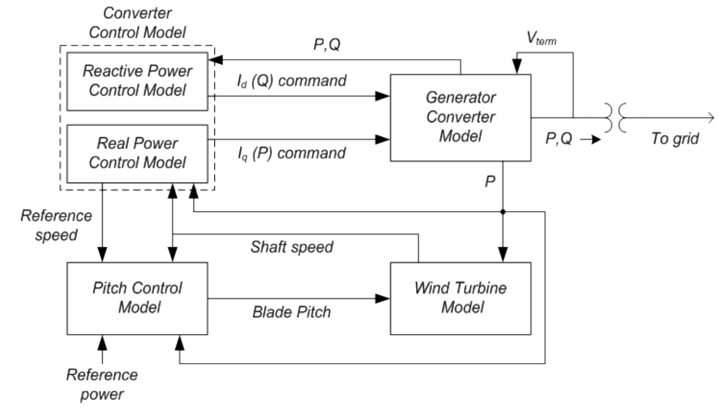

Fig. 2. Schematic of a WECC DFIG WPP model.

The WPP is sized such that the wind penetration level in the two-area system is 10% when the WPP is supplying rated power. The WPP collector system model is represented by an aggregated single-line equivalent. Details on how this aggregation is performed are provided in [16]. The collector system data for the aggregation process is from a real WPP and is presented in [16]. The WECC DFIG WPP model is well documented, and the parameters for the model are available in [17].

C. PVPP Model

The positive sequence dynamic model for PVPP is developed based on the recommendation of the WECC Renewable Energy Modeling Task Force in the detailed report presented in [13]. The dynamic model assumes that the solar irradiance is constant throughout the electrical transient events at the transmission line set by the load flow solution in the pre-fault event. The grid interface is equipped with voltage ride-through capability and current limit to limit the current flow through the power electronics switches (IGBTs).

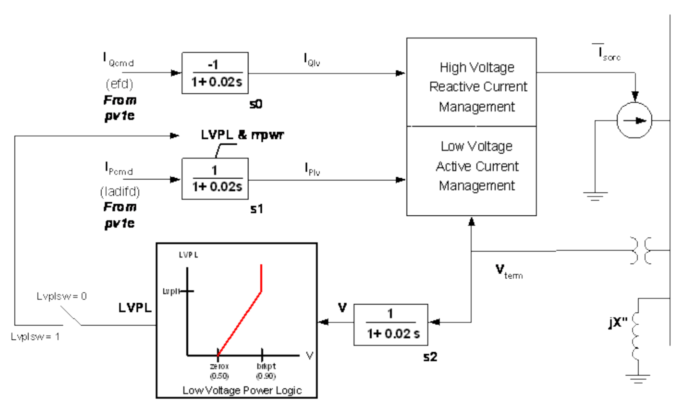

Fig. 3. Block diagram of a PVPP

The dynamic model also represents the capability to limit the ramp rates of the output power injected to the grid and the current limit representing the maximum current-carrying capability of the power electronics switches (IGBT). The output reactive power can be controlled to maintain the voltage, the power factor, or the reactive power generated by the PVPP as implemented in the actual hardware of a PVPP.

D. Oscillation Damping in WPP Controls

Additional WPP controls may be provided by the turbine manufacturer for the purpose of frequency support, but no manufacturer yet offers a dedicated oscillation damping control. Typical frequency support controls include governor droop control and synthetic inertia. Detailed explanations of droop control and synthetic inertia are provided in [18]-[23]. The effects of these controls on oscillation modes are unknown. These controls are not considered in our modeling effort because they are non-standard additions to the WECC WPP model and their effect on modal behavior is debatable.

Oscillation damping controls also differ from frequency support controls in one major aspect: energy injection. The goal of the oscillation damping control is to have a near-zero injection of energy during the time frame of controller action. This means that unlike in the case of frequency support controls, the WPP operator does not suffer much revenue loss during controller action.

In our test case, the WPP is connected at Bus 6 (see Fig. 1) and thus is supplying only Area 1 directly. The WPP output power at the WPP's point of interconnection (Bus 6 in our test case) is measured by the PMU. The damper is tuned to the dominant inter-area modal frequency (0.76 Hz in our test system). When this frequency is observed in the local WPP PMU measurements, the controller is activated.

The implementation of the oscillation damping controller is shown in Fig. 4. The WPP power injected into Bus 6 is our measured variable. Removing the DC component of this power leaves us with the oscillatory component. Applying a notch filter tuned to 0.76 Hz to the oscillatory component allows for the isolation of the dominant oscillation mode. After we see how much the power swing is in this dominant mode, we set the WPP to oppose this mode. We scale down the oscillatory component (so as to not exceed converter ratings for the turbines; more on this in Section V) and add the inverse of this scaled oscillatory component to the reference power command of the WPP. (Fig. 2 shows where this reference power is inputted into the model.) It is expected that the WPP controller will then assign power commands to individual turbines; however, the WECC WPP model does not include individual turbine representations, so individual turbine behavior is not modeled in detail.

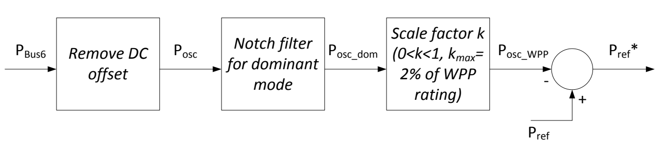

Fig. 4. Control block diagram of oscillation damping control.

For PVPPs, a similar controller can be used if the PVPP is operated off peak (i.e., not at its maximum power point). However, this entails some loss in energy production. For WPPs, a small amount of energy is stored in the rotating masses of the turbine blades and hub that can provide this damping energy even if the turbine is operating at its maximum power point; hence, loss in energy production is negligible. Therefore, we also experimented with a PVPP controller that holds some energy in reserve by operating at a voltage slightly higher than the voltage at the maximum power point.

III. Simulation Cases

Simulations were performed in four configurations with respect to power output level and oscillation damping controller status (enabled or disabled), for both WPPs and PVPPs. The cases are listed in Table I. Each of the synchronous units from Generator (G) 1 through G4 is assumed to be a perfectly coherent representation of multiple synchronous generators. The presence of a WPP or PVPP leads to the displacement of conventional units, hence leading to a reduction in the number of machines comprising a coherent unit. This is represented in our simulation by a reduction in the inertia of coherent unit G2, which is closest to Bus 6, the point of interconnection of the WPP or PVPP. The decision to reduce inertia on this coherent unit to a third of its original value represents the removal of turbogenerators (typical inertia 3 s to 9 s) from a coherent unit, whereas hydro units (typical inertia 2 s) remain [24]. Two WPP and PVPP power output levels were considered: 0.5 pu and 1 pu. If WPP or PVPP power output were to be 0 pu, the provision of the oscillation damping service would be impossible.

TABLE I
List of Cases Based on Wind Power/PV power Output and Damping Controller Status

Case No.	Power Output (pu)	Oscillation Damper Control Status
1	0.5	Disabled
2	0.5	Enabled
3	1.0	Disabled
4	1.0	Enabled

IV. Results

Results from the case studies are presented here. The simulated two-area system is excited by a large disturbance—a breaker connecting an impedance load in parallel to Load 2 located at Bus 9 in Fig. 1 is suddenly switched on. The additional load is 1% of Load 2 in terms of real and reactive power. Signal-processing methods [15] are applied to the resulting electromechanical oscillations to estimate the modal frequency, damping, and the mode shape of the system. The estimated modes for each case are compared to determine if the WPP or PVPP output levels or the controller status influence the system modes.

A. PSD Analysis—Wind

For the case studies, the frequency at each generator bus, the voltage phase angle with respect to the calculated center of angle [9], the voltage phase angle at each generator bus, and the power output at each generator were used to estimate the modes of the system after the power system disturbance was applied. The results of the analysis on the power output at G1 are presented in Fig. 5. The power output signal was selected to analyze modes because the mode estimates were clearest for this signal compared to the voltage phase angle and frequency signals.

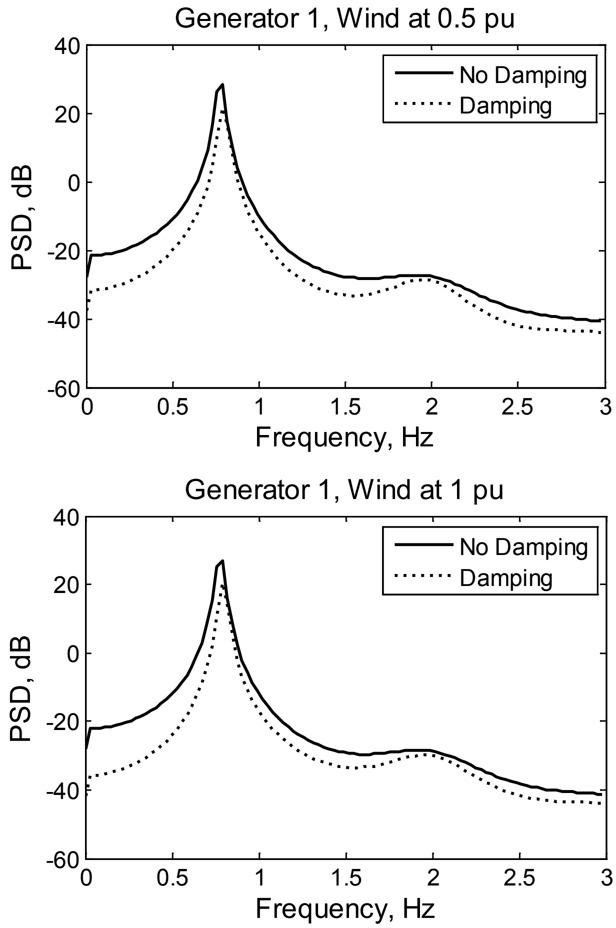

Fig. 5. PSD estimates for the G1 power signal with a WPP.

Fig. 5 shows the significant peaks in the PSD, which indicate that modal frequencies are present in the power output at G1 located at Bus 1 for all cases. The top of Fig. 4 shows the PSD for wind output at 0.5 pu (Case 1 and Case 2). The bottom of Fig 4 shows the PSD for wind output at 1 pu (Case 3 and Case 4). All of these plots indicate the presence of 0.76 Hz, both with the damping controller disabled and with it enabled. This 0.76-Hz frequency falls in the inter-area oscillation range (0.1 Hz to 0.8 Hz) [25], indicating that this frequency is associated with one group of generators oscillating against another group of generators in the system. The presence of the damping controller reduces the peak magnitude of the 0.76-Hz mode by approximately 7 dB when the wind output is at 0.5 pu and by approximately 5 dB when the wind output is at 1 pu. This reduction in the mode's peak magnitude indicates that the damping controller is indeed performing its function. The damping controller cannot eliminate the mode entirely because of the small amount of power that it can supply (limited to 2% of the WPP's rating) compared to the power involved in the inter-area oscillation. The lack of significant additional peaks when wind power is changed from 0.5 pu to 1 pu indicates that the WPP output levels investigated **do not** have a direct impact on the modes of the system. Figs. 6, 7, and 8 show that a similar damping effect is observed at each generator's bus.

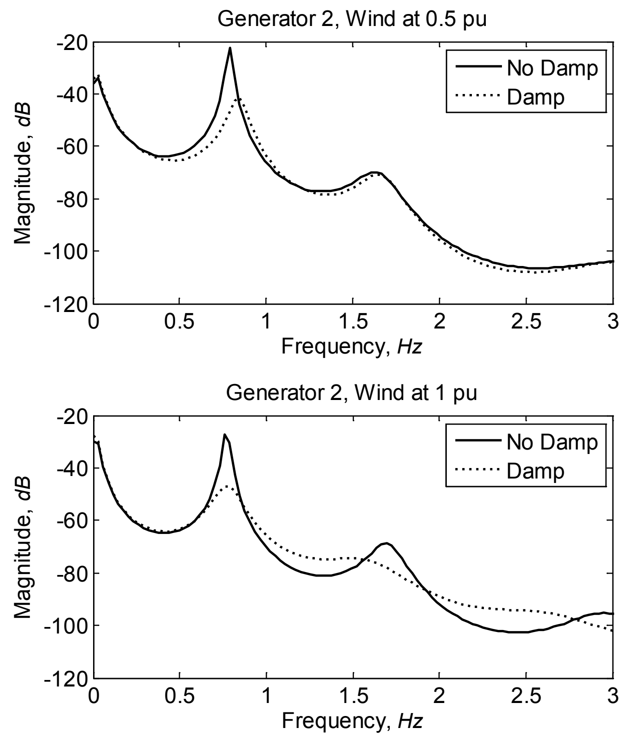

Fig. 6. PSD estimates for the G2 power signal with a WPP.

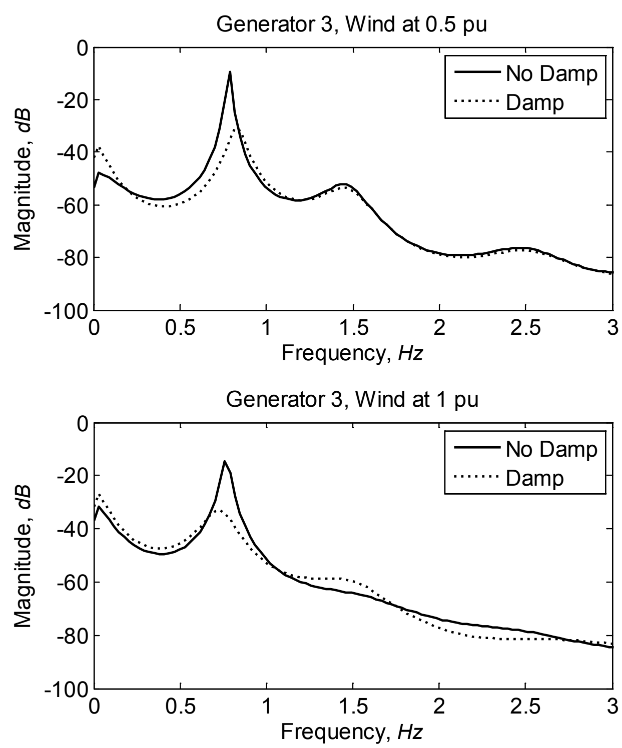

Fig. 7. PSD estimates for the G3 power signal with a WPP.

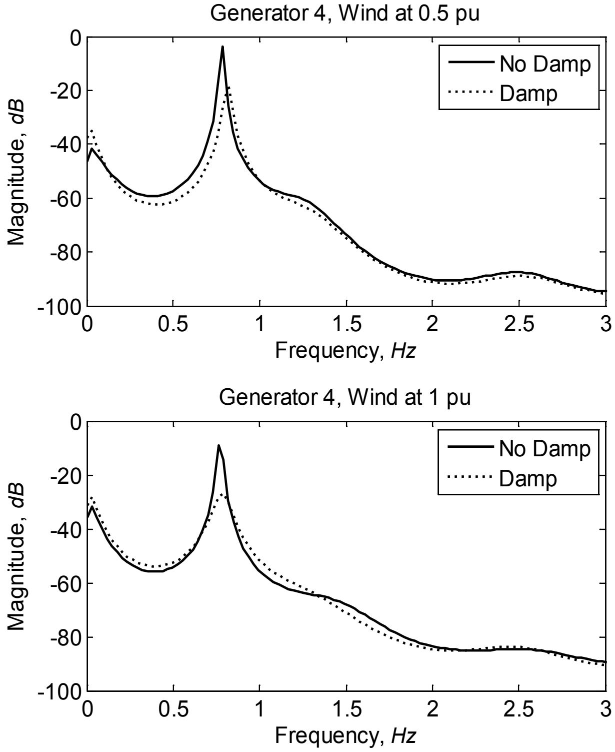

Fig. 8. PSD estimates for the G4 power signal with a WPP.

B. PSD Analysis—Solar

An analysis similar to that performed for a WPP was carried out with a PVPP of similar rating. The same control design was used to provide damping. The plots below (Figs. 9, 10, 11, and 12) show that the PVPP provided some damping for the case when the plant output was 0.5 pu but no damping when the plant output was 1 pu.

When the PVPP was operated at 0.5 pu, the solar insolation was held at 0.55 pu. In our case, 1 pu of solar insolation corresponded to 1,000 W/sq.m., thus 0.55 pu of solar insolation corresponded to 550 W/sq.m. The plant's output was held to 0.5 pu rather than 0.55 pu by operating at a suboptimal point on the current-voltage curve; hence, additional energy available was available (5% of total plant rating) that the controller could use to damp oscillations.
Fig. 9 shows that with the controller in operation and the PVPP at 0.5 pu output, up to 10 dB of damping could be achieved. If a mode were close to the stability margin, this level of damping could be very beneficial. A similar 10 dB damping effect is seen for generators 2, 3 and 4 at 0.5 pu PVPP output in Figures 10, 11 and 12. Note that the oscillation damper does not have to be activated all the time; when an inter-area oscillation is observed, then the PVPP can be temporarily derated to perform the function of oscillation damping until the oscillation disappears, and subsequently operation can be returned to normal. Thus, no energy production is impacted under normal operation.

The plots at each generator bus corroborate the conclusion that the PVPP can provide damping only if there is some power held in reserve. The magnitude of the damping provided is similar to that provided by the WPP; however, a WPP can provide this service in any operating condition. Thus, if this service is provided in the future, WPPs may be better candidates than PVPPs to provide this service. If grid-sized energy storage becomes widespread, storage units may take over this role, depending on the relative locations of the WPPs and the storage units.

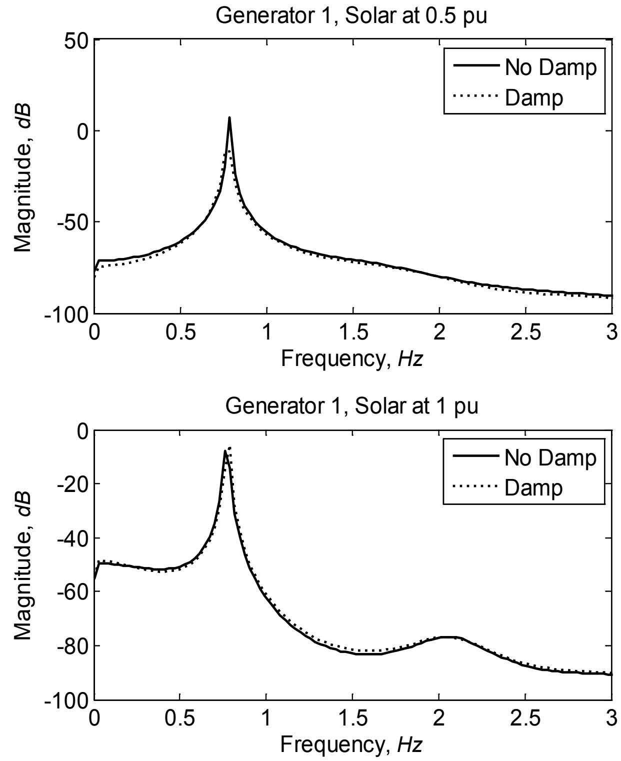

Fig. 9. PSD estimates for the G1 power signal with a PVPP.

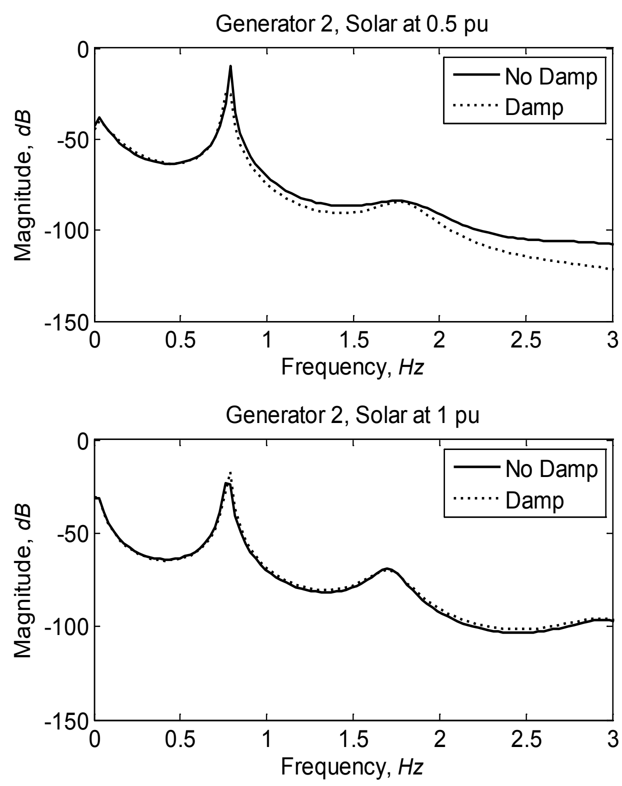

Fig. 10. PSD estimates for the G2 power signal with a PVPP.

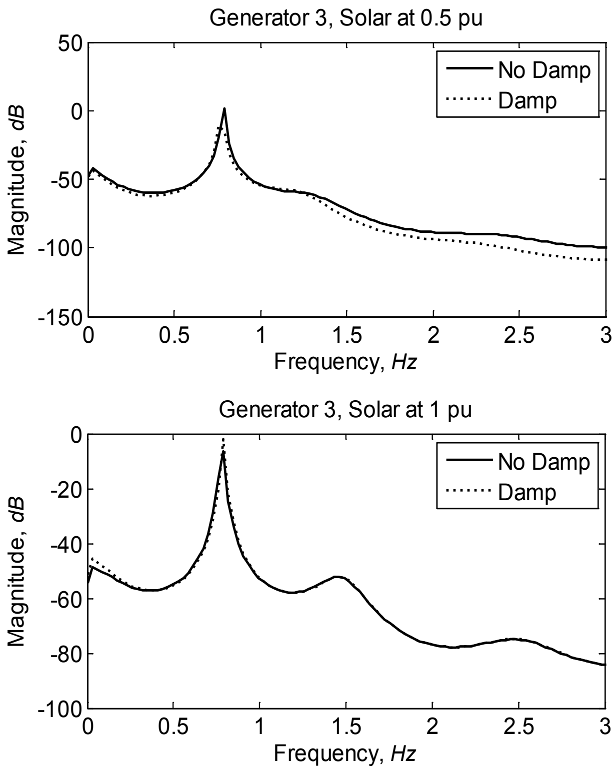

Fig. 11. PSD estimates for the G3 power signal with a PVPP.

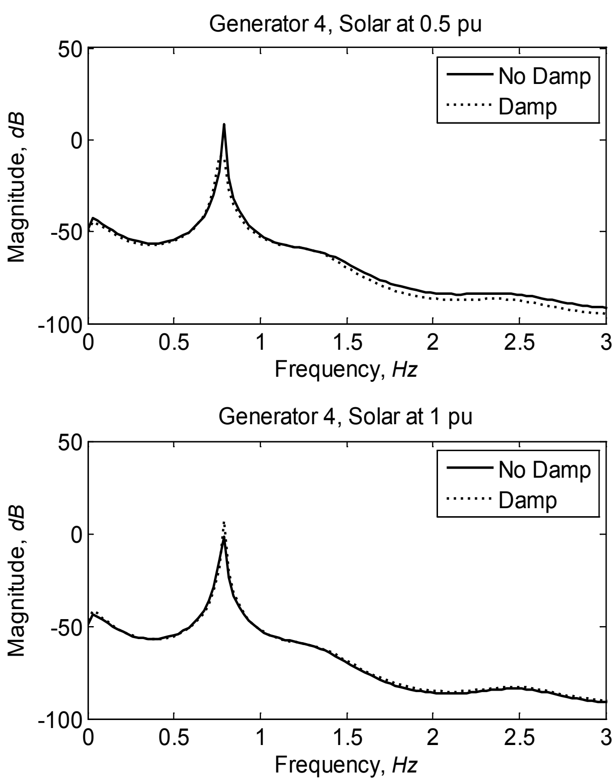

Fig. 12. PSD estimates for the G4 power signal with a PVPP.

V. Conclusion

The work discussed in the full paper indicates that WPPs and PVPPs can make a significant contribution to the damping of inter-area oscillation modes. A controller has been developed that allows WPPs and PVPPs to inject power into the system out of phase with the inter-area oscillation to increase the damping of the oscillation. The controller is able to increase the damping of the oscillation, provided there is some energy available, either in the rotating masses of the WPP or the reserve power held by the PVPP. The reserve power is based on derating the PVPP but it need only be held while the oscillation is occurring, therefore having negligible impact on energy production. Future work will validate these results using archived PMU data from real power systems and using the capabilities of the National Renewable Energy Laboratory's controllable grid interface. In the future, by providing this service, WPPs and PVPPs could play an active role in improving the grid's stability. As VG penetration levels increase, such analyses will become increasingly relevant.

VI. Acknowledgement

This work was supported by the U.S. Department of Energy under Contract No. DE-AC36-08-GO28308 with the National Renewable Energy Laboratory.

VII. References

[1] DOE, "20% wind energy by 2030: Increasing wind energy's contribution to U.S. electricity supply," National Renewable Energy Laboratory, Golden, CO, Tech. Rep., NREL/TP-500-41869, DOE/GO-102008-2567, May 2008. Available: www.nrel.gov/docs/fy08osti/41869.pdf

[2] Electric Reliability Council of Texas, "ERCOT grid operations wind integration report: 05/02/2013," Austin, TX, 2013. Available: http://www.ercot.com/content/gridinfo/generation/windintegration/2013/05/ERCOT%20Wind%20Integration%20Report%2005-02-13.pdf

[3] GE Energy, "Western wind and solar integration study," National Renewable Energy Laboratory, Golden, CO, Subcontract Rep., NREL/SR-550-47434, 2010. Available: http://www.nrel.gov/docs/fy10osti/47434.pdf

[4] N. Miller, M. Shao, and S. Venkataraman, "CAISO frequency response study," GE Energy, Schenectady, NY, 2011. Available: http://www.uwig.org/Report-FrequencyResponseStudy.pdf

[5] J. G. Slootweg and W. L. Kling, "The impact of large-scale wind power generation on power system oscillations," *Elect. Power Syst. Res.*, vol. 67, pp. 9–20, 2003.

[6] G. Tsourakis, B. M. Nomikos, and C. D. Vournas, "Contribution of doubly-fed wind generators to oscillation damping," *IEEE Trans. Energy Conversion*, vol. 24, no. 3, pp. 783, 791, Sept. 2009.

[7] A. Mendonca and J. A. Peas Lopes, "Impact of large-scale wind power integration on small-signal stability," *Future Power Systems, 2005 International Conference on*, Nov. 2005.

[8] D. Gautam, V. Vittal, and T. Harbour, "Impact of increased penetration of DFIG-based wind turbine generators on transient and small-signal stability of power systems," *IEEE Trans. Power Syst.*, vol. 24, no. 3, pp. 1,426, 1,434, Aug. 2009.

[9] P. Kundur, *Power System Stability and Control.* New York: McGraw-Hill, 1974, pp. 814.

[10] Manitoba HVDC Research Centre, "PSCAD/EMTDC: Electromagnetic transients program including dc systems," 1994.

[11] T. K. Das and G. K. Venayagamoorthy, "Optimal design of power system stabilizers using a small population-based PSO," *IEEE Power Engineering Society, General Meeting*, Montreal, Quebec, June 12–16, 2006.

[12] M. Behnke, A. Ellis, Y. Kazachkov, T. McCoy, E. Muljadi, W. Price, and J. Sanchez-Gasca, "Development and validation of WECC variable-speed wind turbine dynamic models for grid integration studies," in *Proc. 2007 WINDPOWER Conf.*, Los Angeles, CA, June 2007.

[13] A. Ellis, M. Behnke, and C. Barker. "PV system modeling for grid planning studies," in *Photovoltaic Specialists Conference (PVSC), 2011 37th IEEE*.
[14] M. Singh and S. Santoso, "Dynamic models for wind turbines and wind power plants," National Renewable Energy Laboratory, Golden, CO, Subcontract Rep., NREL/SR-52780, 2011. Available: http://www.nrel.gov/docs/fy12osti/52780.pdf
[15] J. W. Pierre, D. J. Trudnowski, and M. K. Donnelly, "Initial results in electromechanical mode identification from ambient data," *IEEE Trans. Power Syst.*, vol. 12, no. 3, pp. 1,245–1,251, 1997.
[16] E. Muljadi, C. P. Butterfield, A. Ellis, J. Mechenbier, J. Hocheimer, R. Young, N. Miller, R. Delmerico, R. Zavadil, and J. C. Smith, "Equivalencing the collector system of a large wind power plant," *IEEE Power Engineering Society, General Meeting*, Montreal, Quebec, June 12–16, 2006.
[17] WECC Renewable Energy Modeling Task Force, "WECC wind power plant dynamic modeling guide," 2010. Available: http://renew-ne.org/wp-content/uploads/2012/05/WECCWindPlantDynamicModelingGuide.pdf
[18] G. Lalor, A. Mullane, and M. O'Malley, "Frequency control and wind turbine technologies," *IEEE Trans. Power Syst.*, vol. 20, no. 4, pp. 1,905–1,913, 2005.
[19] G. Ramtharan, J. B. Ekanayake, and N. Jenkins, "Frequency support from doubly-fed induction generator wind turbines," *IET Renew. Power Gen.,* vol. 1, pp. 3–9, 2007.
[20] J. F. Conroy and R. Watson, "Frequency response capability of full-converter wind turbine generators in comparison to conventional generation," *IEEE Trans. Power Syst.*, vol. 23, no. 2, pp. 649, 656, May 2008.
[21] N. R. Ullah, T. Thiringer, and D. Karlsson, "Temporary primary frequency control support by variable-speed wind turbines—Potential and applications," *IEEE Trans. Power Syst.*, vol. 23, no. 2, pp. 601, 612, May 2008.
[22] A. Buckspan, J. Aho, P. Fleming, Y. Jeong, and L. Pao, "Combining droop curve concepts with control systems for wind turbine active power control," *Power Electronics and Machines in Wind Applications (PEMWA), 2012 IEEE*, Denver, CO, July.
[23] J. Morren, S. W. H. De Haan, W. L. Kling, and J. A. Ferreira, "Wind turbines emulating inertia and supporting primary frequency control," *IEEE Trans. Power Syst.*, vol. 21, no. 1, pp. 433, 434, Feb. 2006.
[24] G. Andersson, R. Atmuri, R. Rosenqvist, and S. Torseng, "Influence of Hydro Units' generator-to-turbine inertia ratio on damping of subsynchronous oscillations," *IEEE Trans. Power Apparatus*, vol. PAS-103, no. 8, pp. 2,352, 2,361, Aug. 1984.
[25] M. Klein, G. J. Rogers, and P. Kundur, "A fundamental study of inter-area oscillations in power systems," *IEEE Trans. Power Syst.*, vol. 6, no. 3, pp. 914, 921, Aug. 1991.

VIII. Biographies

Mohit Singh (M'2011) received his M.S. and Ph.D. in electrical engineering from the University of Texas at Austin in 2007 and 2011, respectively. His research focuses on the dynamic modeling of wind turbine generators. Dr. Singh is currently working at the National Renewable Energy Laboratory in Golden, Colorado, USA, as a postdoctoral researcher in transmission and grid integration of renewable energy. His current interests include modeling and testing various applications of wind turbine generators and other renewable energy resources. He is a member of the IEEE, and he is involved in the activities of the IEEE Power and Energy Society.

Alicia Allen (M'2013) received her Ph.D. in electrical engineering from the University of Texas at Austin in 2013. She joined the transmission and grid integration group at the National Renewable Energy Laboratory, in Golden, Colorado, in April 2013. Her current research focuses on power system impacts of the integration of MW-scale wind turbines on the distribution system. Her other research interests include wide-area measurement and control systems, power system protection, and power system stability.

Eduard Muljadi (M'82-SM'94-F'10) received his Ph.D. in electrical engineering from the University of Wisconsin at Madison. From 1988 to 1992, he taught at California State University at Fresno. In June 1992, he joined the National Renewable Energy Laboratory, in Golden, Colorado. His current research interests are in the fields of electric machines, power electronics, and power systems in general, with emphasis on renewable energy applications. He is member of Eta Kappa Nu and Sigma Xi and a fellow of the IEEE. He is involved in the activities of the IEEE Industry Application Society (IAS), Power Electronics Society, and Power and Energy Society (PES). He is currently a member of various committees of the IAS and a member of the Working Group on Renewable Technologies and Dynamic Performance Wind Generation Task Force of the PES. He holds two patents in power conversion for renewable energy.

Vahan Gevorgian (M'97) graduated from the Yerevan Polytechnic Institute (Armenia) in 1986. During his studies, he concentrated on electrical machines. His thesis research dealt with doubly-fed induction generators for stand-alone power systems. He obtained his Ph.D. in electrical engineering from the State Engineering University of Armenia in 1993. His dissertation was devoted to the modeling of electrical transients in large wind turbine generators.

Dr. Gevorgian is currently working at the National Wind Technology Center of the National Renewable Energy Laboratory, in Golden, Colorado, USA, as a research engineer. His current interests include the modeling and testing of various applications of small wind turbine-based power systems.